IEEE Access
Multidisciplinary | Rapid Review | Open Access Journal

SPECIAL SECTION ON MOLECULAR COMMUNICATION NETWORKS

Received December 3, 2018, accepted December 26, 2018, date of publication February 4, 2019, date of current version February 27, 2019.

Digital Object Identifier 10.1109/ACCESS.2019.2897173

Biological Circuits for Detection in MoSK-Based Molecular Communication

MALCOLM EGAN[1], (Member, IEEE), TRUNG Q. DUONG[2], (Senior Member, IEEE), AND MARCO DI RENZO[3], (Senior Member, IEEE)

[1]CITI Laboratory, INSA-Lyon, INRIA, Université de Lyon, 69621 Villeurbanne, France
[2]Institute of Electronics, Communications and Information Technology, Queen's University Belfast, Belfast BT7 1NN, U.K.
[3]Laboratoire des Signaux et Systémes, CNRS, CentraleSupélec, Univ Paris Sud, Université Paris-Saclay, 91192 Gif-sur-Yvette, France

Corresponding author: Malcolm Egan (malcom.egan@inria.fr)

This work was supported in part by the U.K. Engineering and Physical Sciences Research Council under Grant EP/P019374/1 and in part by the Newton Fund Institutional Link through the Fly-by Flood Monitoring Project under Grant ID 428328486, which is delivered by the British Council.

ABSTRACT A key justification for molecular communications is low energy consumption and limited complexity. However, this is only the case if effective architectures for transmitting and receiving devices exist, which is not the case for most modulation and coding schemes at present. One approach to implementing these devices is to use biological circuits, based on chemical reaction networks and DNA transcription processes. In this paper, we develop a biological circuit to demodulate a class of molecular shift keying modulation schemes. A feature of our scheme is that only a single kind of receptor is required to which either of the signaling molecules can bind. We analyze our scheme to tune parameters and compare it to an optimal demodulation scheme. This reveals tradeoffs between performance and complexity in biological circuit implementations.

INDEX TERMS Biological circuits, detection, molecular communication.

I. INTRODUCTION

For communication systems to support biological computing [1], nanoscale sensor networks [2] and lab-on-chip devices [3], there is a need for simple devices with very low energy consumption. To meet these requirements, approaches inspired by nature have been proposed. One such approach is communication exploiting the exchange of information-carrying molecules—known as molecular communications [4]—with information processing carried out using biological circuits [5].

Recently, there has been significant progress in developing biological circuits for transmitters and receivers in molecular communication systems. These include the encoding and decoding circuits in [6], the pulse generators in [7], and the analog demodulation circuits in [8] and [9] for reaction-shift keying.

Despite this rapid progress, none of these circuits are suited to digital communication with more than one type of signaling molecule. As such an approach forms the basis of the popular molecular shift keying (MoSK) modulation scheme [10] (see also the survey in [11]), it is desirable to develop biological circuits for demodulation of this class of modulation schemes. However, any demodulation circuit must account for potential non-specificity of receptors to which signaling molecules bind. That is, it is necessary to account for the possibility that multiple types of signaling molecules are able to bind with each receptor, potentially with different affinities.

In this paper, we view the non-specificity of the receptors as an opportunity. In particular, we propose a scheme based on MoSK, where there is only a single type of receptor. This means that either of the types of signaling molecules are able to bind with any receptor. The key benefit of this approach is potential complexity reductions in fabrication of the receiving device, or a reduction in the total number of required receptors.

Our modulation scheme differs from classical MoSK [11] in that the number of each type of molecule is Poisson distributed, bearing some similarities to the concentration shift keying scheme in [12]. This modulation scheme is more reasonable when it is difficult for the transmitter to guarantee that a fixed number of molecules is produced in a given time period. As such, our approach is applicable when there are time-varying energy constraints or the transmitter molecule production circuit is far from the thermodynamic limit [13].

Our approach exploits a newly developed technique for reconstructing the number of each type of molecules bound

The associate editor coordinating the review of this manuscript and approving it for publication was Daniel Benevides Da Costa.

to each receptor [14]. This technique provides a method to design chemical reaction systems that produce samples from the posterior distribution for the number of each type of species bound to the receiver, given the number of molecules produced by each receptor. By tailoring this method to our MoSK demodulation problem, we are able to solve the hypothesis testing problem for which message was sent.

In particular, with the posterior samples in hand, we develop further chemical reaction systems to output a decision. These chemical reaction systems are inspired by robust adaptation mechanisms that arise in bacteria chemotaxis [15], [16]. Via an analysis of the probability of error, we demonstrate the impact of each parameter in the communication system. We compare the error probability in our scheme with the optimal detection rule for the average Bayes' risk, which reveals insights into the tradeoffs between performance and system complexity.

A key observation from our analysis is that for desirable choices of system parameters, the communication channel closely approximates a binary erasure channel. This is a useful observation as it suggests that recent work on channel coding with small numbers of messages is applicable [17]. In particular, it provides a means of obtaining nearly optimal codes for the probability of error to be reduced to an arbitrarily low level.

The remainder of this paper is organized as follows. In Section II, we introduce our system model. In Section III, we present the concept of chemical reaction networks, which is used extensively throughout the remainder of the paper. In Section V, we analyze the output statistics of our receiver and optimize parameters in order to minimize the symbol error probability for uncoded transmissions. In Section VI, we discuss coding for our demodulator and additional mechanisms that may be required for implementation, as well as open issues. In Section VII, we conclude by highlighting future research directions.

Notation: Vectors are denoted by bold lowercase letters, random vectors by bold uppercase letters, and matrices by bold uppercase sans serif letters (e.g., $\mathbf{x}$, $\mathbf{X}$, $\mathbf{X}$). Chemical species by uppercase upper case sans serif letters (e.g., S) and the concentrations by square brackets (e.g., $[\mathsf{S}]$). We denote the distribution of a random vector $\mathbf{X}$ by $P_{\mathbf{X}}$. The Poisson distribution with intensity parameter $\lambda > 0$ is denoted by $\text{Poiss}(\lambda)$.

II. SYSTEM MODEL

Consider two devices that can emit and detect two chemical species, respectively. Denote the chemical species by S_1 and S_2. The two devices communicate over time slots of duration T by modulating the number of molecules S_1 and S_2 emitted by the transmitter.

Our focus is on binary modulation schemes. At the beginning of each time slot $[\mathsf{S}_1]$ molecules of S_1 and $[\mathsf{S}_2]$ molecules are emitted. In particular, when the message $m = 0$ is to be sent, $[\mathsf{S}_1] \sim \text{Poiss}(\lambda_0)$ and $[\mathsf{S}_2] = 0$. On the other hand, when the message $m = 1$ is to be sent, $[\mathsf{S}_1] = 0$ and $[\mathsf{S}_2] \sim \text{Poiss}(\lambda_1)$.

After entering the fluid medium between the transmitter and receiver, the signaling molecules are transported to the receiver. We assume that each emitted molecule binds to a receptor on the receiver within the time slot duration T with a probability p. Moreover, the events that the molecules bind to a receptor within the time slot are all independent.

We remark that the particular transport process carrying molecules from the transmitter to the receiver is not of significant importance for the purposes of this paper. As long as the probability p is constant and the binding events for each signaling molecule are independent, any transport process can be considered. One important example is diffusion, which can often be modeled by the Wiener process. The probability p is then given by the first hitting time of each molecule. In the case of one dimensional Brownian motion with non-zero drift, the first hitting time is inverse Gaussian distributed [18]. As such, the probability p can be obtained as

$$p = \int_0^T \sqrt{\frac{\lambda}{2\pi u^3}} \exp\left(-\frac{\lambda(u-\mu)^2}{2\mu^2 u}\right) du, \tag{1}$$

where $\mu = \frac{d}{v}$ and $\lambda = \frac{d^2}{\sigma^2}$, with d the distance between the transmitter and the receiver, v the drift velocity and σ^2 the variance of the Wiener process. In the case of anomalous diffusion (e.g., due to turbulence), a Lévy walk may be a more appropriate model [19].

There may also be molecules of $\mathsf{S}_1, \mathsf{S}_2$ naturally in the environment and noise in the reception process. For example, a signaling molecule binds with a receptor more than once due to non-zero reverse reaction rates. The noise consisting either of molecules of species S_1 or S_2, is then modeled by independent Poisson random variables. In particular, the naturally occuring concentrations are S_1 and S_2 is Poisson with intensity λ_Z.

The effect of the channel is to introduce independent thinning for the number of transmitted molecules and the Poisson distributed noise is additive, independent of the input. As such, it follows that the number of molecules of S_1 and S_2 at the receiver, denoted by $[\mathsf{S}_{R,1}]$, $[\mathsf{S}_{R,2}]$ are both Poisson distributed, conditioned on the message m that was transmitted. In particular, the number of binding events, $[\mathsf{S}_{R,1}]$, $[\mathsf{S}_{R,2}]$, during a time slot T have the conditional distributions

$$\begin{aligned} [\mathsf{S}_{R,1}]_{|m=0} &\sim \text{Poiss}(p\lambda_0 + \lambda_Z), \quad [\mathsf{S}_{R,1}]_{|m=1} \sim \text{Poiss}(\lambda_Z) \\ [\mathsf{S}_{R,2}]_{|m=0} &\sim \text{Poiss}(\lambda_Z), \quad [\mathsf{S}_{R,2}]_{|m=1} \sim \text{Poiss}(p\lambda_1 + \lambda_Z). \end{aligned} \tag{2}$$

The goal of this paper is to develop a chemical receiver that produces a distinct chemical signal, depending on which message is detected. The role of the receiver is to output a decision for which mesage was sent, denoted by $\hat{m} \in \{0, 1\}$. A key feature of our model is that we include the impact of non-specific receptors. That is, both the signaling molecules $\mathsf{S}_1, \mathsf{S}_2$ can bind to any receptor on the surface of the receiver, albeit with different affinities.

After a signaling molecule binds with a receptor, molecules of another chemical species Y are produced *inside the receiver*. As such, these molecules can be directly observed and processed to detect the transmitted message. We consider a linear model [14] for the number of molecules of Y that are produced by the binding events during a given time slot. In particular, the number of molecules, $[\mathsf{Y}]$, of Y that are produced is given by

$$[\mathsf{Y}] = o_1[\mathsf{S}_{R,1}] + o_2[\mathsf{S}_{R,2}], \tag{3}$$

where $o_1, o_2 \in \mathbb{Z}_{\geq 0}$. The coefficients o_1, o_2 depend on the affinities of the receptors to $\mathsf{S}_1, \mathsf{S}_2$. If $o_1 > o_2$, the receptor has a higher affinity for S_1 than for S_2.

III. CHEMICAL REACTION NETWORK PRELIMINARIES

Our proposed receiver architecture is implemented by a biological circuit. In order to design the circuit, we require results from chemical reaction network theory. To this end, let $\mathcal{S} = \{\mathsf{X}_1, \ldots, \mathsf{X}_m\}$ be a set of chemical species. Associated with the system is a set of r reactions. For the j-th reaction, let $\boldsymbol{\nu}_j, \boldsymbol{\nu}'_j$ be the vectors in $\mathbb{Z}^m_{\geq 0}$ representing the number of molecules of each species consumed and created, respectively, in one instance of the j-th reaction. The j-th reaction can then be written in the form

$$\sum_{i=1}^{m} \nu_{j,i}\mathsf{X}_i \rightarrow \sum_{i=1}^{m} \nu'_{j,i}\mathsf{X}_i. \tag{4}$$

The set of all chemical reactions is denoted by $\mathcal{R}$.

A complex is a formal linear combination of chemical species; e.g., $\mathsf{X}_1 + 3\mathsf{X}_2$. We denote the set of all complexes defined by $\boldsymbol{\nu}_j, \boldsymbol{\nu}'_j$ by $\mathcal{C}$. A chemical reaction network is then the triple $(\mathcal{S}, \mathcal{C}, \mathcal{R})$.

We will require the notions of both stochastic and deterministic models for the kinetics of chemical reaction networks. The stochastic model will be based on the chemical master equation, which can be well approximated by a deterministic model in the thermodynamic limit [13]. However, in general, the stochastic and deterministic models can significantly differ in their behavior.

The stochastic model for a chemical reaction network $(\mathcal{S}, \mathcal{C}, \mathcal{R})$ specifies the rate of production of each new species. If the j-th reaction occurs at time t, the new state of the system is

$$\mathbf{X}(t) = \mathbf{X}(t-) + \boldsymbol{\nu}'_k - \boldsymbol{\nu}_k, \tag{5}$$

where $\mathbf{X}(t)$ is the random vector of concentrations of each chemical species at time t. Let $R_k(t)$ denote the number of times that the k-th reaction occurs by time t. Then, the state of the system at time t can be written as

$$\mathbf{X}(t) = \mathbf{X}(0) + \sum_k R_k(t)(\boldsymbol{\nu}'_k - \boldsymbol{\nu}_k), \tag{6}$$

where the sum is over all previous reactions.

The process $R_k(t)$ is a counting process [20] with intensity $\lambda_k(\mathbf{X}(t))$ and can be written as

$$R_k(t) = Y_k\left(\int_0^t \lambda_k(\mathbf{X}(s))ds\right), \tag{7}$$

where the Y_k are independent, unit-rate Poisson processes. The intensity functions λ_k are assumed to be of the form

$$\lambda_k(\mathbf{x}) = \kappa_k\left(\prod_{l=1}^{m} \nu_{l,k}!\right)\binom{\mathbf{x}}{k}, \tag{8}$$

which is known as the stochastic mass action model. Note that the concentration trajectories of each chemical species can be obtained using stochastic simulation techniques [21], a fact that we will exploit later to obtain Monte Carlo estimates of error probabilities.

It is clear from (5) that $\mathbf{X}(t)$ forms a Markov chain. A such, it may admit a stationary distribution. In particular, if the reactions are all reversible, a unique stationary distribution $\pi(\mathbf{x})$ exists, given by

$$\pi(\mathbf{x}) = \lim_{t\to\infty} \Pr(\mathbf{X}(t) = \mathbf{x} | \mathbf{X}(0) = \mathbf{y}), \tag{9}$$

for all reachable $\mathbf{x}, \mathbf{y}$.[1]

For the results in the sequel, it is necessary to specify conditions under which this stationary distribution can be characterized. These conditions are given in terms of a deterministic model for the chemical reaction network $(\mathcal{S}, \mathcal{C}, \mathcal{R})$.

Initially, we will focus on a particular class of chemical reaction networks defined by the reactions

$$\begin{aligned} \mathsf{X}_1 &\overset{\kappa_1}{\rightarrow} a\mathsf{X}_2 \\ a\mathsf{X}_2 &\overset{\kappa_2}{\rightarrow} \mathsf{X}_1, \end{aligned} \tag{10}$$

where $a \in \mathbb{Z}_{>0}$.

The concentration of each species $\mathsf{X}_1, \mathsf{X}_2$ is the number of molecules normalized by the volume, V, of the container. In our case, the container is the receiving device. Let $[\mathsf{X}_1](t), [\mathsf{X}_2](t)$ be the concentrations of $s\mathsf{X}_1, \mathsf{X}_2$ at time t, respectively. Deterministic mass-action kinetics of this class of chemical reactions is defined by the system of ordinary differential equations

$$\begin{aligned} \frac{d[\mathsf{X}_1](t)}{dt} &= -\kappa_1[\mathsf{X}_1](t) + \kappa_2[\mathsf{X}_2](t)^a \\ \frac{d[\mathsf{X}_2](t)}{dt} &= -\kappa_2[\mathsf{X}_2](t)^a + \kappa_1[\mathsf{X}_1](t). \end{aligned} \tag{11}$$

Note that this chemical reaction network satisfies the detailed balance condition for any choice of $\kappa_1, \kappa_2 > 0$, and in particular $\kappa_1 = \kappa_2$ which we will assume in all that follows. As a consequence by [20, Th. 4.1], the unique stationary distribution of the reaction network defined by (10) is given by

$$\pi(\mathbf{x}) = M_\Gamma e^{-c_1-c_2}\frac{c_1^{x_1}}{x_1!}\frac{c_2^{x_2}}{x_2!}, \ \mathbf{x} \in \Gamma \tag{12}$$

[1] That is, the number of molecules of each species can take the values in $\mathbf{x}, \mathbf{y}$.

where (c_1, c_2) is a point of detailed balance[2] satisfying the identity $c_1 = c_2^a$, Γ is the irreducible subset of $\mathbb{Z}^2_{\geq 0}$ accessible via the reactions in (10) and M_Γ is a normalizing constant.

When we develop a thresholding scheme within our proposed receiver in the following section, we will require a more general class of chemical reaction networks. However, for the purposes of exposition, we will defer further discussion until Section IV-B.

IV. PROPOSED RECEIVER ARCHITECTURE

In this section, we develop our proposed receiver architecture. There are three stages: sampling from the posterior distribution; demodulation; and the decision rule. The first stage can be viewed as providing an estimate of the true number of each chemical species $\mathsf{S}_1, \mathsf{S}_2$ that bind with the receptors. On the other hand, the second and third stages exploit this estimate in order to make a decision $\hat{m} \in \{0, 1, e\}$, where the estimate e corresponds to an erasure (i.e., no estimate for the symbol is obtained).

A. STAGE 1: SAMPLING FROM THE POSTERIOR

The first stage of the receiver is to obtain partial estimates of the concentrations, $[\mathsf{S}_{R,1}]$, $[\mathsf{S}_{R,2}]$, of $\mathsf{S}_1, \mathsf{S}_2$ on the surface of the receiver. These estimates are obtained via the output of the receptor $[\mathsf{Y}]$, given by

$$[\mathsf{Y}] = a[\mathsf{S}_{R,1}] + [\mathsf{S}_{R,2}]. \tag{13}$$

We seek to sample from the Bayesian posterior

$$P_{[\mathsf{S}_{R,1}],[\mathsf{S}_{R,2}]|[\mathsf{Y}]}(y_1, y_2) \propto P_{[\mathsf{Y}]|[\mathsf{S}_{R,1}],[\mathsf{S}_{R,2}]}(y_R) P_{[\mathsf{S}_{R,1}],[\mathsf{S}_{R,2}]}(y_1, y_2), \tag{14}$$

where $P_{[\mathsf{S}_{R,1}],[\mathsf{S}_{R,2}]}(y_1, y_2)$ is a product-Poisson prior, given by

$$P_{[\mathsf{S}_{R,1}],[\mathsf{S}_{R,2}]}(y_1, y_2) = e^{-2q} \frac{q^{y_1}}{y_1!} \frac{q^{y_2}}{y_2!}. \tag{15}$$

The parameter $q > 0$ is the rate parameter, to be selected.

In order to sample from the posterior in (14), we will use a method recently developed in [14]. Let $\mathsf{X}_1, \mathsf{X}_2$ be two chemical species. The basis of this scheme are the reactions

$$\begin{aligned} \mathsf{X}_1 &\xrightarrow{q} a\mathsf{X}_2 \\ a\mathsf{X}_2 &\xrightarrow{q} \mathsf{X}_1, \end{aligned} \tag{16}$$

where q is the rate parameter in (15). The concentrations at time t are denoted by $[\mathsf{X}_1](t)$ and $[\mathsf{X}_2](t)$, respectively. The reaction will be initialized by $[\mathsf{X}_1](0) = [\mathsf{Y}]$ and $[\mathsf{X}_2](0) = 0$.

It follows from [20, Theorem 4.1] that the unique stationary distribution corresponding to the chemical reaction network in (16) is given by

$$\pi(\mathbf{x}) = M_{L([\mathsf{Y}])} \frac{c_1^{x_1}}{x_1!} \frac{c_2^{x_2}}{x_2!}, \quad \mathbf{x} \in L([\mathsf{Y}]), \tag{17}$$

[2]Note that this point is not necessarily unique. Nevertheless, any point satisfying the detailed balance condition will yield the same stationary distribution [20].

where

$$L([\mathsf{Y}]) = \{\mathbf{x} \in \mathbb{Z}^2_{\geq 0} : ax_1 + x_2 = [\mathsf{Y}]\}. \tag{18}$$

The fact that $\pi(\mathbf{x})$ corresponds to the desired posterior distribution in (14) follows by specializing [14]. As such, in order to sample from the posterior in (14), it is sufficient to observe the chemical reaction network in (16) at a sufficiently large time t. If t is chosen large enough, the observations of $[\mathsf{X}_1](t)$, $[\mathsf{X}_2](t)$ will well approximate samples from (14).

To illustrate the behavior of the chemical reaction network in (16), suppose that $[\mathsf{Y}] = 6$. Assuming that $a = 5$ in (16), the values of $[\mathsf{X}_1](t)$ and $[\mathsf{X}_2](t)$ are plotted in Fig. 1. Observe that $([\mathsf{X}_1](t), [\mathsf{X}_2](t))$ oscillates between $(1, 1)$ and $(6, 0)$. Since $[\mathsf{Y}] = 6$, it follows that $L([\mathsf{Y}]) = \{(x_1, x_2) \in \mathbb{Z}^2_{\geq 0} : a \cdot x_1 + 1 \cdot x_2 = 6\} = \{(1, 1), (0, 6)\}$. As such, the values taken by the concentrations of $[\mathsf{X}_1](t)$ and $[\mathsf{X}_2](t)$ are consistent with $L([\mathsf{Y}])$.

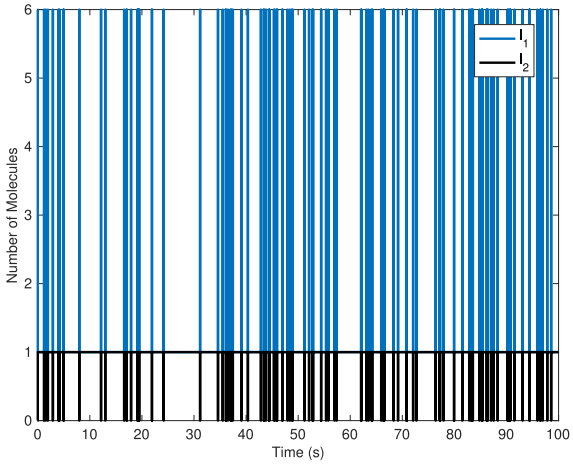

FIGURE 1. Plot of samples with $[\mathsf{Y}] = 6$, $o_1 = 5$, $o_2 = 1$, $q = 1$.

The final component of Stage 1 is to obtain a sample of $[\mathsf{X}_1](t_S)$, $[\mathsf{X}_2](t_S)$ at the desired sampling time t_S. This can be achieved using two transcription activation networks, which has also been applied in the biological circuit-based decoder in [6]. In particular, the sampling circuit consists of a repressor transcription factor and its corresponding corepressor. The corepressors bind to specific sites on transcription factor proteins and produce a steady state concentration of activated transcription factors equal to the concentration of transcription factors, if the initial concentration of corepressors is sufficiently high. Therefore, at the sampling time it is sufficient to inject a large number of corepressors to activate the production of the activated transcription factors corresponing to the species $\mathsf{X}_1, \mathsf{X}_2$. In the steady state, the concentration of the activated transcript factor will be equal to $[\mathsf{X}_1](t_S)$, $[\mathsf{X}_2](t_S)$ at the sampling time.

As noted in [6], the sampling procedure is not instantaneous. In our setting, this can potentially cause a problem when a reaction in (16) occurs shortly after the corepressors are introduced into the system, particularly when a in (16) is large due to the significant changes in the number of

molecules. This remains an open problem and we discuss it further in Section VI. In the following, we assume that the quantities $[\mathsf{X}_1](t_S)$, $[\mathsf{X}_2](t_S)$ have been perfectly sampled.

B. STAGE 2: DEMODULATION

Stage 1 provides a means of sampling from the posterior distribution in (14). Stage 2 produces two signals, one corresponding to each of $\mathsf{S}_1, \mathsf{S}_2$. In particular, as is common in MoSK-based demodulation, a threshold test will be applied to the samples $[\mathsf{X}_1](t_S)$ and $[\mathsf{X}_2](t_S)$.

To apply the thresholding to the signals $[\mathsf{X}_1](t_S)$ and $[\mathsf{X}_2](t_S)$, we will exploit two further chemical reaction networks that form integral feedback controllers. This kind of control system is used to determine if a chemical signal exceeds a given level in a variety of biological systems; most notably bacteria chemotaxis [15], [16].

To illustrate the idea, consider the chemical reaction network

$$\begin{aligned} \mathsf{A} + \mathsf{B} &\xrightarrow{\alpha} 2\mathsf{B} \\ \mathsf{B} &\xrightarrow{\beta} \mathsf{A}, \end{aligned} \tag{19}$$

where B is an unactivated protein and A is the corresponding activated form. Under the deterministic mass action model, the kinetics for this reaction network are given by

$$\begin{aligned} \frac{d[\mathsf{A}](t)}{dt} &= -\alpha[\mathsf{A}](t)[\mathsf{B}](t) + \beta[\mathsf{B}](t) \\ \frac{d[\mathsf{B}](t)}{dt} &= \alpha[\mathsf{A}](t)[\mathsf{B}](t) - \beta[\mathsf{B}](t). \end{aligned} \tag{20}$$

Let $\Theta = [\mathsf{A}](0) + [\mathsf{B}](0)$. Observe that this chemical reaction network satisfies the conservation law $[\mathsf{A}](t) + [\mathsf{B}](t) = \Theta,\ t \geq 0$. As such, the equilibrium solution satisfies

$$\begin{aligned} \alpha[\mathsf{A}]_e[\mathsf{B}]_e &= \beta[\mathsf{B}]_e \\ [\mathsf{A}]_e + [\mathsf{B}]_e &= \Theta, \end{aligned} \tag{21}$$

where $[\mathsf{A}]_e$ and $[\mathsf{B}]_e$ are the equilibrium concentrations of A and B, respectively. Solving these equations yields

$$\begin{aligned} [\mathsf{A}]_e &= \frac{\beta}{\alpha} \\ [\mathsf{B}]_e &= \Theta - \frac{\beta}{\alpha}, \end{aligned} \tag{22}$$

when a positive equilibrium exists. This means that whenever $\Theta > \frac{\beta}{\alpha}$, corresponding to a sufficiently large value of $[\mathsf{B}](0)$, the equilibrium concentration is given by $[\mathsf{A}]_e = \frac{\beta}{\alpha}$.

To illustrate this behavior, Fig. 2 plots the concentration trajectory $[\mathsf{A}](t)$ for different values of $[\mathsf{B}](0)$. In the figure $[\mathsf{A}](0) = 0$. Observe that when $[\mathsf{B}](0)$ exceeds $\frac{\beta}{\alpha} = 2.5$, the equilibrium concentration $[\mathsf{A}]_e = 2.5$, as expected.

We use the reaction network in (19) to produce a chemical signal used to output the decision in Stage 3. In particular we require two reaction networks of the form in (19), with non-interacting chemical species. One of these reaction networks will be applied to X_1 and the other to X_2. The consequence is that when the concentration of $[\mathsf{X}_1](t)$ or $[\mathsf{X}_2](t)$ exceeds $\frac{\beta}{\alpha}$, the reaction network will always output the same value. After sampling using a transcription activation network as in Stage 1, the concentrations of $[\mathsf{A}_1](t'_S)$ and $[\mathsf{A}_2](t'_S)$ at the sampling time t'_S can then be used to obtain an estimate $\hat{m}$.

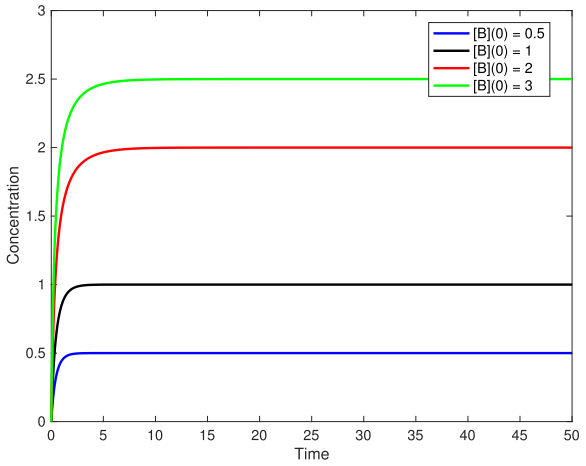

FIGURE 2. Plot of trajectories with $\alpha = 1$, $\beta = 2.5$.

Before presenting Stage 3, we remark that the chemical reaction network in (19) is not the only choice. In general, biological systems use much more complicated integral feedback controllers, such as in [16]. Nevertheless, the key idea behind integral feedback control is the presence of zero-order kinetics. For more details on this more general class of chemical reaction networks see, for example, [22].

C. STAGE 3: DECISION OUTPUT

The final stage is to obtain the estimate $\hat{m}$. This is achieved by observing the two output signals $[\mathsf{A}_1](t'_S)$ and $[\mathsf{A}_2](t'_S)$ from the integral feedback control circuit based on (19). The value of $\frac{\beta}{\alpha}$ is chosen to be equal to the thresholds τ_1, τ_2. Therefore, if the threshold test is passed, the value of $[\mathsf{A}_1](t'_S)$ and $[\mathsf{A}_2](t'_S)$ will be fixed to $\frac{\beta}{\alpha}$. On the other hand, if the input to Stage 2 is below the threshold then one or both of the conditions $[\mathsf{A}_1](t'_S) < \tau$ and $[\mathsf{A}_2](t'_S) < \tau$ will be satisfied.

Observe that it is possible that both $[\mathsf{A}_1](t'_S)$ and $[\mathsf{A}_2](t'_S)$ either exceed or fall below the threshold. In this case, we say that an erasure has occured and the erasure symbol e is output from the detection circuit. To determine whether an erasure has occured, we introduce a third signal (called an erasure signal), which takes a constant value e_1 if an erasure has occured and e_0 otherwise.

The erasure signal can be obtained using the XOR operation, and as such we require an implementation of the XOR logic gate. This is in principle possible by exploiting the XOR biological circuit in [23].

V. PROBABILITY OF ERROR ANALYSIS

In this section, we analyze the probability of error for the proposed receiver. There are a number of parameters that a system designer may tune. These include the molecular weight a in (10), the thresholds τ_1, τ_2, the production intensities λ_0, λ_1

and even potentially the quality of the channel encoded in the probability p. We first obtain and analytical expression for the probability of error in terms of finite sums, which can be easily computed numerically. We then provide numerical results to investigate the effect of each parameter on the probability of error.

Recall that there are three possible estimates obtained from the receiver: $m = 1$; $m = 0$; or an erasure. No error occurs if $m = 0$ and $[\mathsf{A}_1](t_S') > \tau_1$, $[\mathsf{A}_2](t_S') \leq \tau_2$ or $m = 1$ and $[\mathsf{A}_1](t_S') \leq \tau_1 < [\mathsf{A}_2](t_S') > \tau_2$. Under the assumption that the sampling times t_S and t_S' are sufficiently large to well approximate the stationary distribution in Stage 1 and the equilibrium in Stage 2, the probability of successful transmission is well approximated by

$$P_S \approx \frac{1}{2}\Pr([\mathsf{A}_1](t_S') > \tau_1, \quad [\mathsf{A}_2](t_S') \leq \tau_2 | m = 0) + \frac{1}{2}\Pr([\mathsf{A}_1](t_S') \leq \tau_1, \quad [\mathsf{A}_2](t_S') > \tau_2 | m = 1). \quad (23)$$

It follows from the decision rule in Stage 3 of the receiver that the probability a message is correctly detected given $m = 0$ was transmitted is given by

$$\Pr([\mathsf{A}_1](t_S') > \tau_1, [\mathsf{A}_2](t_S') \leq \tau_2 | m = 0) = \sum_{a_1, a_2 \in \mathbb{Z}^2_{\geq 0}} \mathbf{1}_{\{a_1 > \tau_1, a_2 \leq \tau_2\}} \times \Pr([\mathsf{A}_1](t_S') = a_1, [\mathsf{A}_2](t_S') = a_2 | m = 0). \quad (24)$$

Similarly, in the case that $m = 1$ was transmitted, the probability of correctly detecting $\hat{m} = 1$ is given by

$$\Pr([\mathsf{A}_1](t_S') \leq \tau_1, [\mathsf{A}_2](t_S') > \tau_2 | m = 1) = \sum_{a_1, a_2 \in \mathbb{Z}^2_{\geq 0}} \mathbf{1}_{\{a_1 \leq \tau_1, a_2 > \tau_2\}} \times \Pr([\mathsf{A}_1](t_S') = a_1, [\mathsf{A}_2](t_S') = a_2 | m = 1). \quad (25)$$

By using the fact that the output concentrations depend on the stationary distribution of the chemical reaction network in Stage 1, it follows that in the case $m = 0$

$$\begin{aligned}
&\Pr([\mathsf{A}_1] = a_1, [\mathsf{A}_2] = a_2 | m = 0) \\
&= \sum_{y_1, y_2 \in \mathbb{Z}_{\geq}} \pi_{ay_1+y_2}(a_1, a_2) \Pr([\mathsf{S}_{R,1}] = y_1) \Pr([\mathsf{S}_{R,2}] = y_2) \\
&= \sum_{y_1, y_2 \in \mathbb{Z}_{\geq}} \pi_{ay_1+y_2}(a_1, a_2) \\
&\quad \times e^{-p\lambda_0 - \lambda_Z} \frac{(p\lambda_0 + \lambda_Z)^{y_1}}{y_1!} e^{-\lambda_Z} \frac{(\lambda_Z)^{y_2}}{y_2!}. \quad (26)
\end{aligned}$$

Similarly, in the case $m = 1$ we have

$$\begin{aligned}
&\Pr([\mathsf{A}_1] = a_1, [\mathsf{A}_2] = a_2 | m = 1) \\
&= \sum_{y_1, y_2 \in \mathbb{Z}_{\geq}} \pi_{ay_1+y_2}(a_1, a_2) \Pr([\mathsf{S}_{R,1}] = y_1) \Pr([\mathsf{S}_{R,2}] = y_2) \\
&= \sum_{y_1, y_2 \in \mathbb{Z}_{\geq}} \pi_{ay_1+y_2}(a_1, a_2) \\
&\quad \times e^{-\lambda_Z} \frac{(\lambda_Z)^{y_1}}{y_1!} e^{-p\lambda_1 - \lambda_Z} \frac{(p\lambda_1 + \lambda_Z)^{y_2}}{y_2!}. \quad (27)
\end{aligned}$$

The probability measure $\pi_z(x_1, x_2)$ is obtained from the stationary distribution for the stochastic chemical reaction network in Stage 2. To obtain an explicit representation of $\pi_z(x_1, x_2)$, note that

$$L(z) = \{(x_1, x_2) \in \mathbb{Z}^2_{\geq 0} : ax_1 + x_2 = z\}. \quad (28)$$

The stationary distribution is then given by [14]

$$\pi_z(x_1, x_2) = \left\{ \begin{array}{ll} \frac{1}{K} e^{-2q} \frac{q^{x_1} q^{x_2}}{x_1! x_2!}, & (x_1, x_2) \in L(z) \\ 0, & \text{otherwise,} \end{array} \right\} \quad (29)$$

with normalization constant

$$K = \sum_{(x_1, x_2) \in L(z)} e^{-2q} \frac{q^{x_1} q^{x_2}}{x_1! x_2!}. \quad (30)$$

Fig. 3 shows the probability of error for varying molecular weight a in Stage 1. Observe that the analytical approximation of the probability of the error obtained from (23) is in good agreement with the probability of error obtained from Monte Carlo simulations. For small values of a, the probability of error is very high, and in fact greater than 0.5 since errors due to erasures can occur. The high probability of error is due to the fact that when $[\mathsf{Y}] < a$, the true values of $[\mathsf{S}_{R,1}]$, $[\mathsf{S}_{R,2}]$ can be perfectly reconstructed. However, in the case $[\mathsf{Y}] \geq a$, there is more than one element of $L([\mathsf{Y}])$ in (18). As such an error can occur, with probability depending on the choice of the prior distribution in (15). Therefore, it is desirable to make a as large as possible, subject to constraints on the available chemical species used to implement the reaction network.

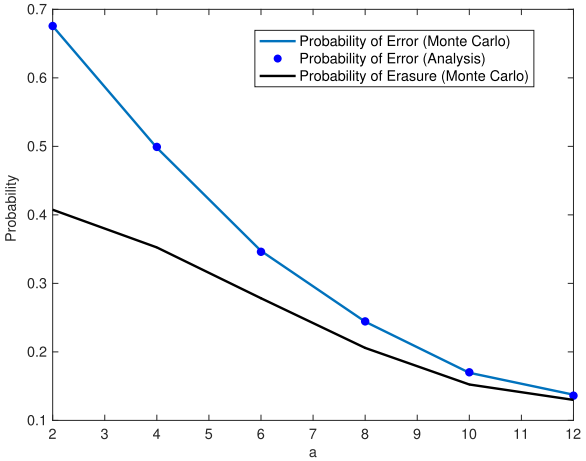

FIGURE 3. Probability of error for varying molecular weight a. The parameters for the simulation are: $p = 0.9$; $\lambda_Z = 1$; $\lambda_0 = 6$; $\lambda_1 = 6$; $\tau_1 = 2$; $\tau_2 = 2$.

Fig. 3 also demonstrates that for a sufficiently large value of a, the probability that an erasure occurs very closely approximates the probability of error. That is, almost all errors are in fact erasures. This is a useful observation from

the perspective of designing channel codes, which we discuss further in Section VI.

Fig. 4 shows the effect of changing the intensity parameter for the Poisson distribution governing the number of molecules that are transmitted. A key observation is that a large intensity $\lambda = \lambda_0 = \lambda_1$ does not improve the probability of error. The key reason for this is that as more molecules are transmitted, the number of molecules $[\mathsf{Y}]$ produced by the receptors also increases. As noted in the discussion of Fig. 3, this can result in imperfect reconstruction of $[\mathsf{S}_{R,1}]$, $[\mathsf{S}_{R,2}]$. As such, the error probability increases. On the other hand, for small values of λ, there is a higher probability that $[\mathsf{S}_{R,1}]$ or $[\mathsf{S}_{R,2}]$ contain no information about the transmitted signal as only noise is present. Therefore it is desirable to optimize the choice of λ to minimize the probability of error.

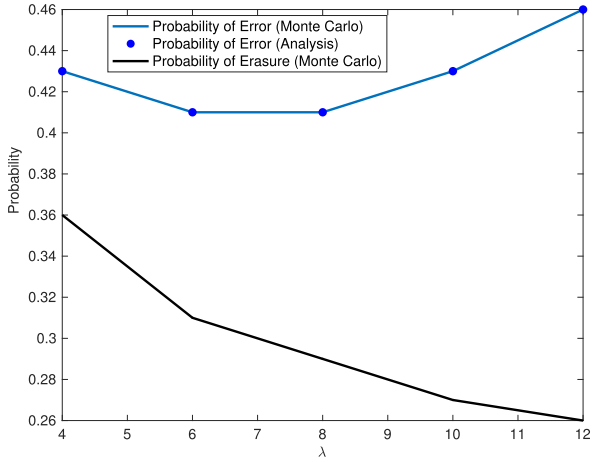

FIGURE 4. Probability of error for varying $\lambda_0 = \lambda_1 = \lambda$. The parameters for the simulation are: $p = 0.9$; $\lambda_Z = 1$; $a = 5$; $\tau_1 = \tau_2 = 2$.

Fig. 4 also shows the erasure probability. For small values of λ, the erasure probability better approximates the actual probability of error. Again, this is a desirable feature from the perspective of channel coding, discussed further in Section VI.

VI. DISCUSSION

In this section, we discuss limitations of the receiver design and methods to improve the performance. In particular, we first compare our design with the optimal decision procedure. We show that the optimal decision scheme is more challenging to implement within a biological circuit, albeit with the benefit of lower error probabilities. To remedy this problem, we discuss channel coding schemes suitable for the molecular communication regime. Finally, we discuss some practical implementation issues.

A. COMPARISON WITH OPTIMAL DECISIONS

Based on samples $[\mathsf{A}_1](t'_S)$, $[\mathsf{A}_2](t'_S)$, we seek to obtain the optimal decision rule in the sense that the average Bayes' risk is minimized. Let $\mathcal{H}_0$ be the hypothesis that $m = 0$ and $\mathcal{H}_1$ be the hypothesis that $m = 1$. It follows immediately from the likelihood ratio test [24] that the optimal decision rule is given by

$$\Pr([\mathsf{A}_1](t'_S), [\mathsf{A}_2](t'_S)|m = 1) \underset{\mathcal{H}_0}{\overset{\mathcal{H}_1}{\gtrless}} \Pr([\mathsf{A}_1](t'_S), [\mathsf{A}_2](t'_S)|m = 0). \quad (31)$$

Note that

$$\begin{aligned}\Pr([\mathsf{A}_1](t'_S), [\mathsf{A}_2](t'_S)|m = 1) &= \sum_{y_1,y_2\in\mathbb{Z}_{\geq 0}} \pi_{L(y_1+ay_2)}([\mathsf{A}_1](t'_S), [\mathsf{A}_2](t'_S)) \\ &\quad \times e^{-\lambda_Z}\frac{(\lambda_Z)^{y_1}}{y_1!} e^{-p\lambda_1-\lambda_Z}\frac{(p\lambda_1+\lambda_Z)^{y_2}}{y_2!} \quad (32)\end{aligned}$$

and

$$\begin{aligned}\Pr([\mathsf{A}_1](t'_S), [\mathsf{A}_2](t'_S)|m = 0) &= \sum_{y_1,y_2\in\mathbb{Z}_{\geq 0}} \pi_{L(y_1+ay_2)}([\mathsf{A}_1](t'_S), [\mathsf{A}_2](t'_S)) \\ &\quad \times e^{-p\lambda_0-\lambda_Z}\frac{(p\lambda_0+\lambda_Z)^{y_1}}{y_1!} e^{-\lambda_Z}\frac{(\lambda_Z)^{y_2}}{y_2!}. \quad (33)\end{aligned}$$

Table 1 compares the performance of the proposed scheme and the optimal scheme in (31). The system parameters correspond to: $\lambda = \lambda_0 = \lambda_1 = 4$; $p = 0.9$; $\lambda_Z = 1$; $\tau_1 = \tau_2 = 2$, $q_1 = q_2 = 1$. As expected, the optimal scheme admits a lower probability of error, with roughly a factor of 3 improvement over our scheme albeit with the need for more complex computations. As can be inferred from Fig. 4, a significant proportion of the error contribution is due to the presence of erasures in our scheme. Due to the challenge of implementing the rule in (31), it may be more desirable to instead introduce error control coding. We examine this approach next.

TABLE 1. Probability of error for the proposed scheme and optimal detection for varying a in (19).

a	Scheme in Section IV	Optimal Detection
5	0.43	0.16
7	0.31	0.11
10	0.24	0.07

B. CODING SCHEMES

In Section V, we observed that for parameter choices that lead to lower probabilities of error, the probability of error is dominated by the probability of erasure. As a consequence, the communication channel in this setting can be approximated by an erasure channel. It is therefore of interest to understand how channel coding might be performed.

In molecular communications, the symbol period, T, is typically long due to the slow transportation of molecules from the transmitter to the receiver. As such, letting the blocklength $n \to \infty$ may not be a desirable approach. Recently, there has been significant interest in fundamental limits of communication in the finite blocklength regime. Perhaps the most well known work is the second order asymptotic approach developed in [25], which yields bounds on the rate in terms of the blocklength and channel parameters.

Another approach is to fix the number of messages M as well as the blocklength n, and then find an optimal code. This approach has been studied by Lin *et al.* in [17]. For the erasure channel with a maximum likelihood decoder, they have shown that the class of weak flip codes (which are in general non-linear) are optimal in the sense that the probability of error is minimized.

The work by Lin *et al.* can be adopted in our work with $M = 2$ messages to reduce the probability of error. In this case, the optimal code with a blocklength n (i.e., n symbols are transmitted) is the flip code of type t for any $t \in \{0, \ldots, \lfloor n/2 \rfloor\}$ given by

$$\mathcal{C} = \begin{pmatrix} 0 & \cdots & 0 & 1 & \cdots & 1 \\ 1 & \cdots & 1 & 0 & \cdots & 0 \end{pmatrix}, \tag{34}$$

where each row of $\mathcal{C}$ corresponds to a codeword (i.e., $m \in \{0, 1\}$) with t ones on the first row. Note that for $t = 0$, this corresponds to a repetition code. For $M > 2$, more general classes of weak flip codes are optimal (see [17]).

Due to the high degree of structure in (the generally non-linear) weak flip codes, it is an interesting problem to develop encoders and decoders implemented via biological circuits. This would lead to an end-to-end communication system analogous to the recent work in [6], which focused on the class of linear block codes.

C. ON IMPLEMENTATION

While we have developed a general structure for receivers with a MoSK modulation scheme, there remain issues that need to be addressed to obtain a working implementation. We briefly highlight three key issues that we believe form important future work:

Issue 1 (Receptor Design): We have seen the important role that the choice of o_1, o_2 plays in the error probability. In particular, when $o_1 = a$ and $o_2 = 1$, choosing a large a leads to significant improvements in the probability of error. It is therefore desirable to design the receptors on the surface of the receiver such that a is as large as possible. Another option is to adjust the choice of information-carrying molecules. However, there is a tradeoff between the resulting affinities to the receptor, the ease of production and the probability that a given molecule can be successfully transported to the receiver.

Issue 2 (Leakage): A challenge when designing biological circuits with a number of chemical species is ensuring that there are no couplings. That is, there are no unintended chemical reactions. The presence of this kind of leakage depends on the particular chemical species in the design of the system. In general, there will be different times scales and quantities of molecules involved in the reactions for Stage 1 and Stage 2. Therefore, some kinds of leakage will have a significantly higher impact than others.

Issue 3 (Sampling Limitations): In both Stage 1 and Stage 2, sampling was implemented using transcription activation networks. As also noted in Section IV, these reactions do not occur instanteneously and therefore if there are changes in concentrations, the sampler may behave erroneously. It is therefore a key question to develop sampling schemes that account for the reaction rates in stochastic chemical reaction networks, as well as the rate of reactions in transcript activation networks.

VII. CONCLUSION

A key difficulty in developing practical molecular communication systems, particularly targeted at nanoscale networking, is designing transmitter and receiver architectures. In this paper, we have explored solutions to this problem using biological circuits based on chemical reaction networks and DNA transcription.

In particular, we considered demodulation of a signal obtained from a class of molecular shift keying schemes. An important feature of our approach is that only a single kind of receptor on the surface of the receiver is required to which both signaling molecules can bind. By analyzing the probability of error, we obtain insights into effective choices of the parameters and comparisons with the optimal detection strategy.

We also discuss how the error probability can be used with channel coding strategies recently introduced for communication systems with a small number of messages. An interesting research direction is therefore to also develop a biological circuit for encoding and decoding, similar to recent work by Marcone *et al.* in [6] for a different class of channel codes with provable optimality.

A further direction is to investigate the behavior of our proposed communication strategy in the presence of an external biological system. This leads to the problem of coexistence, which we have recently investigated in [26] and [27]. In particular, the choice of modulation scheme should be adjusted to satisfy a divergence constraint [27] or the species corresponding to the information-carrying molecules should fall in a restricted class [26]. Minimizing the probability of error subject to these additional constraints in the MoSK-based scheme proposed in this paper currently remains an open problem.

REFERENCES

[1] P. Beckett and A. Jennings, "Towards nanocomputer architecture," *Austral. Comput. Sci. Commun.*, vol. 24, no. 3, pp. 141–150 2002.

[2] I. F. Akyildiz, M. Pierobon, S. Balasubramaniam, and Y. Koucheryavy, "The Internet of bio-nano things," *IEEE Commun. Mag.*, vol. 53, no. 3, pp. 32–40, Mar. 2015.

[3] N. Farsad, A. W. Eckford, S. Hiyama, and Y. Moritani, "On-chip molecular communication: Analysis and design," *IEEE Trans. Nanobiosci.*, vol. 11, no. 3, pp. 304–314, Sep. 2012.

[4] T. Nakano, A. W. Eckford, and T. Haraguchi, *Molecular Communication*. Cambridge, U.K.: Cambridge Univ. Press, 2013.

[5] C. J. Myers, *Engineering Genetic Circuits*. Boca Raton, FL, USA: CRC Press, 2010.

[6] A. Marcone, M. Pierobon, and M. Magarini, "Parity-check coding based on genetic circuits for engineered molecular communication between biological cells," *IEEE Trans. Commun.*, vol. 66, no. 12, pp. 6221–6236, Dec. 2018.

[7] Y. Deng, M. Pierobon, and A. Nallanathan, "A microfluidic feed forward loop pulse generator for molecular communications," in *Proc. IEEE Global Commun. Conf. (GLOBECOM)*, Dec. 2017, pp. 1–7.

[8] C. T. Chou. (2018). "Designing molecular circuits for approximate maximum a posteriori demodulation of concentration modulated signals." [Online]. Available: https://arxiv.org/abs/1808.01543
[9] H. Awan and C. T. Chou, "Generalized solution for the demodulation of reaction shift keying signals in molecular communication networks," *IEEE Trans. Commun.*, vol. 65, no. 2, pp. 715–727, Feb. 2017.
[10] H. ShahMohammadian, G. G. Messier, and S. Magierowski, "Optimum receiver for molecule shift keying modulation in diffusion-based molecular communication channels," *Nano Commun. Netw.*, vol. 3, no. 3, pp. 183–195, 2012.
[11] N. Farsad, H. B. Yilmaz, A. Eckford, C.-B. Chae, and W. Guo, "A comprehensive survey of recent advancements in molecular communication," *IEEE Commun. Surveys Tuts.*, vol. 18, no. 3, pp. 1887–1919, 3rd Quart., 2016.
[12] R. Mosayebi, H. Arjmandi, A. Gohari, M. Nasiri-Kenari, and U. Mitra, "Receivers for diffusion-based molecular communication: Exploiting memory and sampling rate," *IEEE J. Sel. Areas Commun.*, vol. 32, no. 12, pp. 2368–2380, Dec. 2014.
[13] D. T. Gillespie, "The deterministic limit of stochastic chemical kinetics," *J. Phys. Chem. B*, vol. 113, no. 6, pp. 1640–1644, 2009.
[14] M. V. Virinchi, A. Behera, and M. Gopalkrishnan, "A stochastic molecular scheme for an artificial cell to infer its environment from partial observations," in *Proc. Int. Conf. DNA-Based Comput.*, 2017, pp. 82–97.
[15] U. Alon, M. G. Surette, N. Barkai, and S. Leibler, "Robustness in bacterial chemotaxis," *Nature*, vol. 397, no. 6715, pp. 168–171, 1999.
[16] G. Shinar and M. Feinberg, "Structural sources of robustness in biochemical reaction networks," *Science*, vol. 327, pp. 1389–1391, Mar. 2010.
[17] H.-Y. Lin, S. M. Moser, and P.-N. Chen, "Weak flip codes and their optimality on the binary erasure channel," *IEEE Trans. Inf. Theory*, vol. 64, no. 7, pp. 5191–5218, Jul. 2018.
[18] K. V. Srinivas, A. W. Eckford, and R. S. Adve, "Molecular communication in fluid media: The additive inverse Gaussian noise channel," *IEEE Trans. Inf. Theory*, vol. 58, no. 7, pp. 4678–4692, Jul. 2012.
[19] T. C. Mai, M. Egan, T. Q. Duong, and M. Di Renzo, "Event detection in molecular communication networks with anomalous diffusion," *IEEE Commun. Lett.*, vol. 21, no. 6, pp. 1249–1252, Jun. 2017.
[20] D. F. Anderson, G. Craciun, and T. G. Kurtz, "Product-form stationary distributions for deficiency zero chemical reaction networks," *Bull. Math. Biol.*, vol. 72, no. 8, pp. 1947–1970, 2010.
[21] D. T. Gillespie, "Exact stochastic simulation of coupled chemical reactions," *J. Phys. Chem.*, vol. 81, no. 25, pp. 2340–2361, 1977.
[22] T.-M. Yi, Y. Huang, M. I. Simon, and J. Doyle, "Robust perfect adaptation in bacterial chemotaxis through integral feedback control," *Proc. Nat. Acad. Sci. USA*, vol. 97, no. 9, pp. 4649–4653. 2000.
[23] A. Goñi-Moreno, M. Amos, and F. de la Cruz, "Multicellular computing using conjugation for wiring," *PLoS ONE*, vol. 8, no. 6, p. e65986, 2013.
[24] V. H. Poor, *An Introduction to Signal Detection and Estimation*. New York, NY, USA: Springer, 1994.
[25] Y. Polyanskiy, H. V. Poor, and S. Verdú, "Channel coding rate in the finite blocklength regime," *IEEE Trans. Inf. Theory*, vol. 56, no. 5, pp. 2307–2359, May 2010.
[26] M. Egan, T. C. Mai, T. Q. Duong, and M. Di Renzo, "Coexistence in molecular communications," *Nano Commun. Netw.*, vol. 16, pp. 37–44, Jun. 2018.
[27] M. Egan, V. Loscri, T. Duong, and M. Di Renzo, "Strategies for coexistence in molecular communication," *IEEE Trans. Nanobiosci.*, to be published.

MALCOLM EGAN (S'10–M'14) received the Ph.D. degree in electrical engineering from the University of Sydney, Australia, in 2014. He was with the Laboratoire de Mathématiques, Université Blaise Pascal, France, and also with the Department of Computer Science, Czech Technical University in Prague, Czech Republic. He is currently an Assistant Professor in CITI, a joint laboratory between INRIA, INSA Lyon, Université de Lyon, France. His research interests include information theory and statistical signal processing with applications in wireless and molecular communications.

TRUNG Q. DUONG (S'05–M'12–SM'13) received the Ph.D. degree in telecommunications systems from the Blekinge Institute of Technology, Sweden, in 2012. From 2013 to 2017, he was a Lecturer (Assistant Professor) with Queen's University Belfast, U.K., where he has been a Reader (Associate Professor), since 2018. He has authored or co-authored more than 300 technical papers published in scientific journals (181 articles) and presented at international conferences (130 papers). His current research interests include the Internet of Things, wireless communications, molecular communications, and signal processing.

Dr. Duong was a recipient of the Best Paper Award at the IEEE Vehicular Technology Conference (VTC-Spring), in 2013, the IEEE International Conference on Communications, in 2014, the IEEE Global Communications Conference, in 2016, and the IEEE Digital Signal Processing Conference, in 2017. He was also a recipient of the Prestigious Royal Academy of Engineering Research Fellowship, from 2016 to 2021, and the Prestigious Newton Prize, in 2017. He currently serves as an Editor for the IEEE TRANSACTIONS ON WIRELESS COMMUNICATIONS, the IEEE TRANSACTIONS ON COMMUNICATIONS, *IET Communications*, and a Lead Senior Editor for the IEEE COMMUNICATIONS LETTERS.

MARCO DI RENZO (S'05–A'07–M'09–SM'14) was born in L'Aquila, Italy, in 1978. He received the Laurea *(cum laude)* and Ph.D. degrees in electrical engineering from the University of L'Aquila, Italy, in 2003 and 2007, respectively, and the Habilitation á Diriger des Recherches (D.Sc.) degree from University Paris-Sud, France, in 2013. Since 2010, he has been a Chargé de Recherche CNRS (CNRS Associate Professor) with the Laboratory of Signals and Systems, CNRS, CentraleSupélec, Univ Paris Sud, Université Paris-Saclay, Paris, France. He is a Senior Member of the IEEE. He was a recipient of several awards, including, the 2013, IEEE-COMSOC Best Young Researcher Award for Europe, Middle East, and Africa, the 2013, NoE-NEWCOM# Best Paper Award, from 2014 to 2015, the Royal Academy of Engineering Distinguished Visiting Fellowship, the 2015, IEEE Jack Neubauer Memorial Best Systems Paper Award, from 2015 to 2018, the CNRS Award for Excellence in Research and Ph.D. Supervision, the 2016, MSCA Global Fellowship (declined), the 2017, SEE-IEEE Alain Glavieux Award for outstanding results in developing several mathematical abstractions (for mobile network modeling), innovating ideas, and demonstrating their usefulness in future wireless communication systems, the 2018, IEEE COMSOC Best Young Professional Award in Academia for outstanding contributions to the academia in terms of innovative Communications Research, and IEEE ComSoc Services, especially in the area of emerging physical-layer technologies, and seven conference Best Paper Awards (2012 and 2014, IEEE CAMAD, 2013, IEEE VTC-Fall, 2014, IEEE ATC, 2015, IEEE ComManTel, 2017, IEEE SigTelCom, and 2018, INISCOM). He serves as an Associate Editor-in-Chief of the IEEE COMMUNICATIONS LETTERS, and as an Editor of the IEEE TRANSACTIONS ON COMMUNICATIONS, and the IEEE TRANSACTIONS ON WIRELESS COMMUNICATIONS. He is a Distinguished Lecturer of the IEEE Vehicular Technology Society and the IEEE Communications Society.